This is a repository copy of *Inferring a difference in the star-forming properties of lower versus higher X-ray luminosity AGNs*.

White Rose Research Online URL for this paper:
http://eprints.whiterose.ac.uk/143432/

Version: Published Version

Article:
Bernhard, E. orcid.org/0000-0001-9227-7346, Grimmett, L.P., Mullaney, J.R. orcid.org/0000-0002-3126-6712 et al. (3 more authors) (2019) Inferring a difference in the star-forming properties of lower versus higher X-ray luminosity AGNs. Monthly Notices of the Royal Astronomical Society: Letters, 483 (1). L52-L57. ISSN 1745-3925

https://doi.org/10.1093/mnrasl/sly217

This article has been accepted for publication in Monthly Notices of the Royal Astronomical Society: Letters ©: 2018 The Authors. Published by University Press on behalf of the Royal Astronomical Society. All rights reserved.

Reuse
Items deposited in White Rose Research Online are protected by copyright, with all rights reserved unless indicated otherwise. They may be downloaded and/or printed for private study, or other acts as permitted by national copyright laws. The publisher or other rights holders may allow further reproduction and re-use of the full text version. This is indicated by the licence information on the White Rose Research Online record for the item.

Takedown
If you consider content in White Rose Research Online to be in breach of UK law, please notify us by emailing eprints@whiterose.ac.uk including the URL of the record and the reason for the withdrawal request.

eprints@whiterose.ac.uk
https://eprints.whiterose.ac.uk/

Monthly Notices
of the
ROYAL ASTRONOMICAL SOCIETY

MNRAS **483,** L52–L57 (2019)
Advance Access publication 2018 November 28

doi:10.1093/mnrasl/sly217

Inferring a difference in the star-forming properties of lower versus higher X-ray luminosity AGNs

E. Bernhard [1]★ L. P. Grimmett,[1] J. R. Mullaney,[1] E. Daddi [2] C. Tadhunter[1] and S. Jin [2,3]

[1]*Department of Physics and Astronomy, University of Sheffield, Sheffield S3 7RH, UK*
[2]*CEA, IRFU, DAp, AIM, Université Paris-Saclay, Université Paris Diderot, Sorbonne Paris Cité, CNRS, F-91191 Gif-sur-Yvette, France*
[3]*School of Astronomy and Space Science, Nanjing University, Nanjing 210093, China*

Accepted 2018 November 14. Received 2018 November 2; in original form 2018 August 24

ABSTRACT

We explore the distribution of $R_{\rm MS} \equiv {\rm SFR/SFR_{MS}}$ (where $\rm SFR_{MS}$ is the star formation rate of 'main-sequence' star-forming galaxies) for AGN hosts at $z = 1$. We split our sample into two bins of X-ray luminosity divided at $L_X = 2 \times 10^{43}$ erg s^{-1} to investigate whether the $R_{\rm MS}$ distribution changes as a function of AGN power. Our main results suggest that, when the $R_{\rm MS}$ distribution of AGN hosts is modelled as a log-normal distribution (i.e. the same shape as that of MS galaxies), galaxies hosting more powerful X-ray AGNs (i.e. $L_X > 2 \times 10^{43}$ erg s^{-1}) display a narrower $R_{\rm MS}$ distribution that is shifted to higher values compared to their lower L_X counterparts. In addition, we find that more powerful X-ray AGNs have SFRs that are more consistent with that of MS galaxies compared to lower L_X AGNs. Despite this, the mean SFRs (as opposed to $R_{\rm MS}$) measured from these distributions are consistent with the previously observed flat relationship between SFR and L_X. Our results suggest that the typical star-forming properties of AGN hosts change with L_X, and that more powerful AGNs typically reside in more MS-like star-forming galaxies compared to lower L_X AGNs.

Key words: galaxies: active – galaxies: evolution – galaxies: statistics – X-rays: galaxies.

1 INTRODUCTION

It is now recognised that the activity caused by the growth of supermassive black holes (SMBHs) at the centre of galaxies [observed as active galactic nuclei (AGNs)] has played a major role in shaping today's galaxies (e.g. Gebhardt et al. 2000; King 2003). However, although there are multiple lines of empirical evidence showing that SMBH growth is *on average* related to the growth of their host galaxy via star formation (see Harrison 2017, for a review), there is no clear consensus on the physical mechanisms (should it be, e.g. feedback or common fuel-triggering mechanism) that generate these trends between average SMBH and galaxy growth.

To better understand the impact of SMBH growth in galaxy evolution, one can measure the star formation rate (SFR) of a large sample of AGN hosts at multiple epochs. Using HERSCHEL,[1] which provides an unprecedented view of the galaxy star formation at far-infrared (FIR) wavelengths, recent studies have found that (1) there is no relationship between mean SFR and X-ray luminosity (L_X, a proxy for AGN power, e.g. Stanley et al. 2015; Lanzuisi et al. 2017; Stanley et al. 2017) and (2) that the mean AGN host SFR is broadly consistent with that of normal star-forming galaxies (e.g. Mullaney et al. 2012; Stanley et al. 2015) for which the SFR is correlated to the stellar mass via the main sequence (MS; e.g. Schreiber et al. 2015, hereafter S15). However, although HERSCHEL provides the deepest view of SFRs at FIR wavelengths, a large fraction of AGN hosts (typically more than 50 per cent) are not individually detected, meaning most studies rely on methods such as stacking to obtain averages. As these averages can potentially be dominated by bright outliers, the empirical mean SFR of AGNs might not be representative of the 'typical' SFRs of the full AGN sample, increasing the complexity of investigating the AGN–galaxy connection (e.g. Mullaney et al. 2015; Scholtz et al. 2018).

Instead of relying on mean SFRs, Mullaney et al. (2015; hereafter M15) have measured the full distribution of SFRs relative to that of the MS ($R_{\rm MS} \equiv {\rm SFR/SFR_{MS}}$) for AGN hosts out to $z \sim 4$ using a combination of HERSCHEL and ALMA observations. They found that the mean average of the $R_{\rm MS}$ distribution is consistent with that of the MS, yet the mode (i.e. the most common value) lies below that of the MS. This is a consequence of the mean being enhanced by bright outliers, leading to a biased picture. Furthermore, they report an $R_{\rm MS}$ distribution for AGN hosts twice as broad as that of MS star-forming galaxies, demonstrating that the star-

★ E-mail: e.p.bernhard@sheffield.ac.uk

[1]HERSCHEL is an ESA space observatory with science instruments provided by European-led Principal Investigator consortia and with important participation from NASA.

© 2018 The Author(s)
Published by Oxford University Press on behalf of the Royal Astronomical Society

Downloaded from https://academic.oup.com/mnrasl/article-abstract/483/1/L52/5212788 by University of Sheffield user on 07 March 2019

forming properties of AGN hosts are more diverse than that of MS galaxies. However, interestingly, they do not find any evidence of a significant evolution of the $R_{\rm MS}$ distribution with redshift. More recently, Scholtz et al. (2018) have measured the distribution of specific SFRs (SFRs relative to stellar masses; sSFRs) for massive (i.e. $M_* > 2 \times 10^{10}\,{\rm M}_\odot$) galaxies hosting bright (i.e. $L_X > 10^{43}$ erg s^{-1}) AGNs in a large range of redshifts (i.e. $1.5 < z < 3.2$), and find good agreement with that of simulated galaxies taken from the EAGLE simulation (see Scholtz et al. 2018, and references therein). They report no differences in the distribution of sSFR with L_X for AGNs with $L_X > 10^{43}$ erg s^{-1}. As demonstrated in Scholtz et al. (2018), while the sSFR distribution hints important information regarding the connection between AGN and their host galaxies, it lacks of context in terms of the MS of star-forming galaxies. Instead, the $R_{\rm MS}$ distribution and how it changes with L_X provide a better insight of the star-forming properties of AGN hosts within this context of the MS of star-forming galaxies.

In this work, we propose to expand upon M15 and measure whether the $R_{\rm MS}$ distribution changes with L_X. As there is no apparent evidence of the $R_{\rm MS}$ distribution evolving with redshift (M15), we focus on AGNs at $z = 1$ (i.e. close to the peak of activity for both SMBH accretion and SFR; Aird et al. 2015). We describe our sample selection and sample properties in Section 2. We present our analysis in Section 3, the results of which are shown in Section 4. The implications of our results are discussed in Section 5, and we conclude in Section 6. Throughout, we adopt a WMAP–7 year cosmology (Larson et al. 2011) and a Chabrier (2003) initial mass function (IMF) when calculating stellar masses and SFRs.

2 SAMPLE SELECTION AND PROPERTIES

Our sample of X-ray sources is from the catalogue of Marchesi et al. (2016) that provides absorption-corrected 2–10 keV L_X for AGNs in the COSMOS field. We only retain sources that have $0.8 < z < 1.2$ to probe AGNs around $z = 1$ and minimize the effect of the SFR evolution with redshift (S15). We find that 776 AGNs in Marchesi et al. (2016) satisfy this requirement (∼75 per cent of which have spectroscopic redshifts), among which 664 are also covered by HERSCHEL observations. We further remove 123 X-ray sources out of the 664 that have upper limits on their intrinsic X-ray luminosities as they mostly affect the lower luminosity range (i.e. $L_X \sim 10^{42–43}$ erg s^{-1}) and could be associated with star formation activity. We show in the top panel of Fig. 1 the distribution of L_X for our full sample of 541 AGNs. We match these X-ray AGNs to the catalogue of Jin et al. (2018) that contains 'superdeblended' IR photometry (i.e. at 24, 100, 160, 250, 350, and 500 μm) for the COSMOS field measured using a method outlined in Liu et al. (2018). Of these, we find that 100 (i.e. ∼18 per cent) show no detection in any of these IR wavelengths. For each of these, we derive 3σ upper limits[2] at 100 and 160 μm using the COSMOS maps provided by the PACS Evolutionary Probe team (Lutz et al. 2011). Our final sample of X-ray selected AGNs contains 541 sources with IR detections in at least one of the following bands: 24 μm (81 per cent), 100 μm (21 per cent), 160 μm (15 per cent), 250 μm (35 per cent), 350 μm (22 per cent), and 500 μm (7 per cent), or upper limits at 100 and 160 μm.

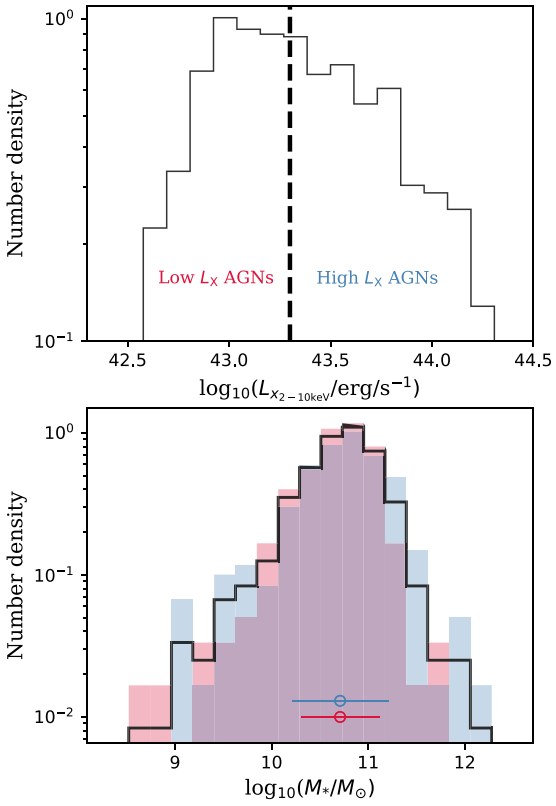

Figure 1. *Top*: The normalized distribution of intrinsic X-ray luminosities for our full sample of AGNs. The dashed vertical line shows our limit for lower and higher L_X AGNs. *Bottom*: The normalized distribution of stellar masses for our full sample of AGNs (black line), our low L_X sample (red histogram), and our high L_X sample (blue histogram). The red and blue circles indicate the positions of the median masses for the low and high L_X samples, respectively, along with their 1σ uncertainties.

To measure SFRs, we use a similar approach than that of Bernhard et al. (2016) which employs multicomponent IR spectral energy distribution (SED) fitting using DECOMPIR[3] (Mullaney et al. 2011). Briefly, DECOMPIR performs chi-square minimization to select the best combination of one out of five templates for the host galaxy emission[4] and an empirically derived AGN template (see Bernhard et al. 2016 and references therein for details on the fitting approach). The IR luminosities arising from star formation are then derived from the fits (after removing the AGN contamination), and converted to SFRs using equation (4) in Kennicutt (1998) adapted for a Chabrier (2003) IMF. This fitting approach is applied to the 30 per cent of our sources that have IR SEDs with at least three photometric points. For the remaining 70 per cent of the sources, we derive SFR upper limits by only fitting the host galaxy templates (i.e. ignoring AGN contamination) using DECOMPIR when the AGN is only detected in two photometric bands, or by using the most common of DECOMPIR templates (i.e. 'SB2') found for our sample with multiple detections, and for which we choose the

[2]The 1σ upper limits are estimated using the standard deviation of a flux distribution built by performing 100 times aperture photometry on randomly selected positions located within the full width at half maximum of the point spread function. The aperture corrections are publicly available at http://www.mpe.mpg.de/resources/PEP/DR1_tarballs/readme_PEP_global.pdf.

[3]DECOMPIR is publicly available at https://sites.google.com/site/decompir/.

[4]See Mullaney et al. (2011) for a full description of the galaxy templates that are available in DECOMPIR.

Downloaded from https://academic.oup.com/mnrasl/article-abstract/483/1/L52/5212788 by University of Sheffield user on 07 March 2019

highest normalization that does not overpredict any detected photometric points or upper limits at 100 and 160 μm. These are SFR upper limits since, should the IR be contaminated by AGN emission, it would decrease the contribution of the host to the IR luminosities, hence SFRs. As our aim is to measure the distribution of SFRs for AGNs relative to that of the MS, we also require host stellar masses. These are derived using CIGALE [5] that performs a multicomponent ultraviolet-to-IR SED fits accounting for AGN contamination (Noll et al. 2009; Ciesla et al. 2015), and shown in the bottom panel of Fig. 1. Our stellar mass estimation is fully presented in Grimmett et al. (submitted). However, as the stellar masses in CIGALE can be affected by contamination from unobscured AGNs (Ciesla et al. 2015), we also performed our analysis using only obscured AGNs (representing roughly 60 per cent of our full sample). In doing so, we find consistent results compared to using the full sample, suggesting that our results are robust to any biases in our mass estimation. The SFR of the MS is derived using equation (9) of S15 adapted for a Chabrier (2003) IMF.

To explore how the distribution of the star-forming properties of AGN hosts changes with L_X, we split our sample of X-ray selected AGNs in two bins of L_X separated at $L_X = 2 \times 10^{43}$ erg s^{-1}, which we refer to as the low and high L_X samples. This cut was chosen to return similar numbers of AGNs between the low and high L_X samples. Overall, our low L_X sample contains 271 sources (50 per cent of the full sample), of which 206 (76 per cent of the low L_X sample) have SFR upper limits and 189 (70 per cent of the low L_X sample) have spectroscopic redshifts, while our high L_X sample contains 270 sources (50 per cent of the full sample) of which 187 (69 per cent of the high L_X sample) have SFR upper limits and 219 (81 per cent of the high L_X sample) have spectroscopic redshifts.

3 MEASURING THE $R_{\rm MS}$ DISTRIBUTION

We now have a sample of 541 X-ray selected AGNs at $z = 1$ separated into bins of low and high L_X and for which we have constraints (in terms of detections or upper limits) of SFRs and stellar masses. However, the presence of a large number of SFR upper limits (∼70 per cent) prevents us from directly deriving the distribution of SFRs. Instead, following M15, we assume that the distribution of SFRs relative to that of the MS (SFR/SFR$_{\rm MS}$ ≡ $R_{\rm MS}$) follows a log-normal distribution as observed for star-forming galaxies (e.g. Sargent et al. 2012; S15), and for which the probability density function (PDF) is defined as

$$\mathrm{PDF} = \frac{1}{\sqrt{2\pi}\,\sigma} \times \exp\left(-\frac{(\log_{10}(R_{\rm MS}) - \mu)^2}{2\sigma^2}\right), \quad (1)$$

where μ and σ are the mean and the standard deviation of the logarithm of $R_{\rm MS}$, respectively. As suggested by M15, this assumption is to ease comparison between the $R_{\rm MS}$ distribution of AGN hosts and MS star-forming galaxies. We perform maximum likelihood estimation (MLE) to find the parameters μ and σ that best fit the observed $R_{\rm MS}$ distributions for both the low and high L_X samples (see Fig. 3 top panel). We use an MLE framework as it allows us to incorporate SFR upper limits (see Grimmett et al. submitted). Due to the complexity of our likelihood function, it cannot be maximized analytically. As a consequence, we maximize it by randomly sampling the posterior distributions of μ and σ employing the affine invariant ensemble sampler of Goodman & Weare (2010) fully implemented into EMCEE[6] (Foreman-Mackey et al. 2013). The benefit of this is that we obtain best-fitting values with meaningful uncertainties that fully account for the presence of a large number of upper limits. We use flat (bounded) prior distributions and check the posterior distributions to verify that they are not constrained in any way by the choice of our prior distributions. The median value of the posterior distribution is taken as the best-fitting parameter, and the standard deviation as its 1σ uncertainty.

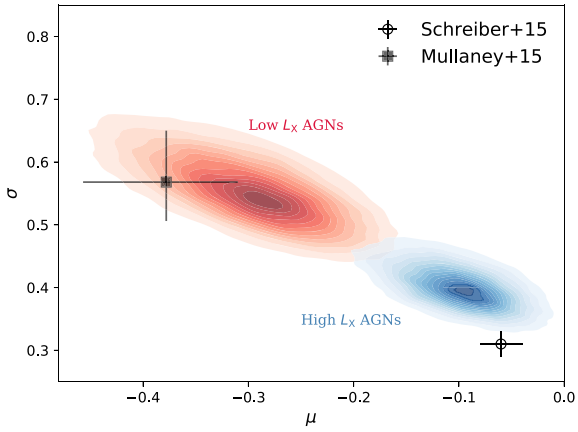

Figure 2. The bivariate distributions of μ and σ resulting from the MLE and that define our $R_{\rm MS}$ distribution (see equation 1) at $z = 1$ split between low (red) and high (blue) L_X AGNs. The full contours show the 1σ spread in each case. We also show the result from M15 for AGN hosts at $z < 1.5$ and that of the MS of galaxies of S15. We find that the parameters that define the $R_{\rm MS}$ distribution of higher L_X AGNs are more consistent with the MS than lower L_X AGNs.

4 RESULTS

4.1 The distributions of $R_{\rm MS}$ ≡ SFR/SFR$_{\rm MS}$

In this work, we explore how the distribution of AGN host SFRs relative to that of the MS for galaxies of S15 changes with L_X at $z = 1$. To do this, we define $R_{\rm MS}$ ≡ SFR/SFR$_{\rm MS}$ as the relative distance from the MS and derive its distribution assuming a log-normal shape with parameters μ and σ (i.e. similar to that of MS galaxies) split between low- and high-L_X AGNs (separated at $L_X = 2 \times 10^{43}$ erg s^{-1}). Within this assumption, we find that the parameters μ and σ for the low and high L_X samples show differences (see Table 1) and that their likelihood distributions peak at different locations in the μ–σ parameter space (see Fig. 2). In particular, our results suggest that the $R_{\rm MS}$ distribution of higher L_X AGNs is *narrower* (i.e. smaller σ by a factor of 1.4) than that of lower L_X AGNs (see Fig. 2), indicating less diversity in the star-forming properties of higher L_X AGN hosts. We also find that the $R_{\rm MS}$ distribution of higher L_X AGN hosts peaks at a higher value of $R_{\rm MS}$ (i.e. higher μ by a factor of 3) than that of lower L_X AGNs (see Fig. 2). These can also be seen in the bottom panel of Fig. 3 where we show the $R_{\rm MS}$ distributions for low- and high-L_X AGN hosts.

In the context of the MS for star-forming galaxies of S15, we find that, while assuming that the $R_{\rm MS}$ distribution of AGN hosts follows a log-normal distribution, the parameters μ and σ of higher L_X AGNs are more consistent with those reported for the MS when compared to lower L_X AGNs at $z \sim 1$ (see Fig. 2). This suggests

[5]CIGALE is publicly available at https://cigale.lam.fr.

[6]EMCEE is publicly available at http://dfm.io/emcee/current/.

Downloaded from https://academic.oup.com/mnrasl/article-abstract/483/1/L52/5212788 by University of Sheffield user on 07 March 2019

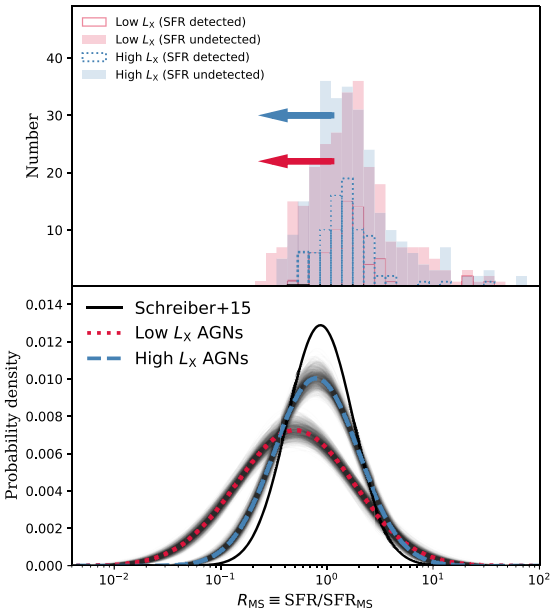

Figure 3. *Top*: The observed R_{MS} distributions split between low- and high-L_X AGNs (see keys). The arrows indicate the presence of upper limits. *Bottom*: The optimized PDFs of R_{MS} split between low (red dotted line) and high (blue dashed line) L_X AGNs. The uncertainties on the PDFs are shown with 500 black thin lines generated by randomly varying μ and σ around their 1σ uncertainties. We also show the R_{MS} distribution of the MS for star-forming galaxies as reported in S15. We find that the R_{MS} distribution of higher L_X AGNs is narrower and closer to that of the MS of galaxies than that of the lower L_X AGNs.

Table 1. The results of the MLE performed to find μ and σ that best fit the observed R_{MS} distributions for our low and high L_X sample of AGNs. Associated errors on each parameter are the 1σ uncertainties measured from the posterior distributions (see Section 3). We also show results for the AGN sample at $z < 1.5$ of Mullaney et al. (2015) and for the MS of star-forming galaxies of Schreiber et al. (2015).

Sample	μ mean of $\ln(R_{MS})$	σ std. dev. of $\ln(R_{MS})$
This work	$-0.30^{\pm0.06}$	$0.55^{\pm0.05}$
Low-L_X AGNs	–	–
This work	$-0.10^{\pm0.04}$	$0.40^{\pm0.03}$
High-L_X AGNs	–	–
All AGNs ($z < 1.5$)	$-0.38^{+0.07}_{-0.08}$	$0.6^{\pm0.1}$
(Mullaney et al. 2015)	–	–
Main sequence	$-0.06^{\pm0.02}$	$0.31^{\pm0.02}$
(Schreiber et al. 2015)	–	–

that the R_{MS} distribution for higher L_X AGNs is in better agreement with that of MS star-forming galaxies when compared to lower L_X AGNs (see Fig. 3 bottom panel), and that therefore higher L_X AGNs at $z \sim 1$ are more likely to reside in MS star-forming galaxies than lower L_X AGNs. However, interestingly, this does not prevent a large fraction of galaxies hosting lower L_X AGNs from experiencing star formation at a level consistent with MS galaxies (e.g. with $R_{MS} > 0.4$; see Fig. 3 bottom panel). This is a consequence of the broader R_{MS} distribution for lower L_X AGNs. Finally, we also find that our results are broadly consistent with those of M15, who performed a similar analysis but for AGNs with $z < 1.5$, complemented with ALMA data, and not split between low- and high-L_X AGNs (see Fig. 2).

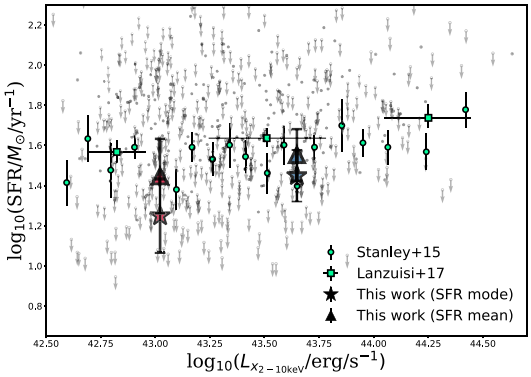

Figure 4. The relationship between SFR and L_X at $z = 1$. The stars show our SFR modes at lower and higher L_X. The triangles show these of our SFR means. The error bars on the mean and the mode are from propagating the uncertainties found on the parameters μ and σ (see Table 1). We also show the observed flat relationship found at similar redshift as reported in Stanley et al. (2015) and Lanzuisi et al. (2017; see bottom right-hand keys). The grey dots indicate the individual SFRs (undetected sources are shown with a downward arrow).

4.2 The relationship between SFR and L_X

We have explored the star-forming properties of AGNs at $z = 1$ by measuring the R_{MS} distribution for low- and high-L_X AGN hosts, assuming that it has the shape of that of MS galaxies (see Section 3). Our results indicate that galaxies hosting higher L_X AGNs have *typical* SFRs consistent with MS star-forming galaxies, in contrast to galaxies hosting lower L_X AGNs.

That the distribution of R_{MS} differs between lower and higher L_X AGNs apparently contradicts recent findings of a flat relationship between SFR and L_X (e.g. Stanley et al. 2015; Lanzuisi et al. 2017). We investigate this apparent contradiction by measuring both the mean[7] R_{MS}^{mean} and the mode[8] R_{MS}^{mode} of the R_{MS} distributions for low- and high-L_X AGNs using our best fit of μ and σ (see Table 1). Knowing SFR_{MS} for each host, we are able to derive the mean and the mode SFR for low- and high-L_X AGNs. We show in Fig. 4 that our average SFRs are in agreement with recent studies that find a flat relationship between SFR and L_X (e.g. Stanley et al. 2015; Lanzuisi et al. 2017). However, as expected, our mode SFRs systematically lie below our mean SFRs, since the means are affected by bright outliers. The reason why our mean SFRs are in better agreement with the flat relationship reported by, e.g. Stanley et al. (2015), is that they use stacking analysis to account for undetected sources which is, in essence, on-image mean-averaging. We further find that the difference between our mode and mean SFRs changes with L_X. This is a consequence of the broader R_{MS} distribution of galaxies hosting lower L_X AGNs. We stress that the differences between the mean and the mode SFR of our L_X bins are consistent within the 1σ error bars derived from propagating the uncertainties found in the parameters μ and σ that define our R_{MS} distribution (see Table 1).

[7]The mean is defined as $R_{MS}^{mean} = \exp(\mu + \sigma^2/2)$.
[8]The mode is defined as $R_{MS}^{mode} = \exp(\mu - \sigma^2)$.

Downloaded from https://academic.oup.com/mnrasl/article-abstract/483/1/L52/5212788 by University of Sheffield user on 07 March 2019

5 DISCUSSION

In this work, we investigate the $R_{\rm MS} \equiv {\rm SFR/SFR_{MS}}$ distribution at $z = 1$ of AGNs split in two bins of L_X separated at $L_X = 2 \times 10^{43}$ erg s^{-1}, and assuming that it follows a log-normal distribution, as found for that of MS star-forming galaxies (e.g. S15). Our results hint that the $R_{\rm MS}$ distributions for low- and high-L_X AGNs are different. In particular, we suggest that the $R_{\rm MS}$ distribution of higher L_X AGN hosts is narrower than that of lower L_X AGNs, which is equivalent to there being less diversity in the host star-forming properties of higher L_X AGNs (see Section 4.1). We propose that the diversity of SFRs in lower L_X AGNs is a consequence of the relative ease for a galaxy to trigger a lower luminosity AGN, as suggested by the large relative number of low-L_X AGNs as opposed to high-L_X AGNs in the X-ray luminosity functions (e.g. Aird, Coil & Georgakakis 2017). In addition, within our assumptions, the $R_{\rm MS}$ distribution of higher L_X AGNs is in better agreement with that of MS galaxies. This could indicate the necessity of a significant amount of gas (i.e. enough to sustain MS host SFRs) to trigger luminous X-ray AGNs.

Our sample contains a large number of SFR upper limits. Yet, our MLE approach fully accounts for this effect by providing sensible uncertainties, and shows that, with the current level of SFR detections at $z \sim 1$ using FIR wavelength, it is likely that lower and higher L_X AGNs have different $R_{\rm MS}$ distributions (i.e. see Fig. 2). If confirmed, the larger agreement between the $R_{\rm MS}$ distribution for higher L_X AGNs with that of the MS of star-forming galaxies suggests a stronger link between SMBH and galaxy growth for powerful AGNs. That is, the concurrence of a higher L_X AGN – indicating ongoing SMBH growth – with a less diverse, more MS-like star-forming host galaxy – suggesting host galaxy growth. The similar galaxy mass distributions between our low and high L_X samples (see the bottom panel of Fig. 1) allow us to make such a direct link between average L_X and average SMBH accretion rate by using the specific L_X (i.e. L_X/M_*) as a proxy for Eddington ratio (see Bernhard et al. 2018, and references therein). In this context, our results are consistent with recent studies that find that the SMBH accretion rate changes with the host galaxy properties (e.g. Kauffmann & Heckman 2009; Georgakakis et al. 2014; Wang et al. 2017; Aird, Coil & Georgakakis 2018a,b; Bernhard et al. 2018; Grimmett et al. submitted). Furthermore, the finding of an $R_{\rm MS}$ distribution for higher L_X AGNs in better agreement with MS galaxies is also consistent with results showing that quasar-like AGN activity is often found in star-forming galaxies (e.g. Rosario et al. 2013; Kalfountzou et al. 2014; Stanley et al. 2017).

Finally, we note that our results hold (i.e. narrower distribution for higher L_X AGNs) when only considering galaxies with stellar masses $M_* > 10^{10}$ M$_\odot$ as is often used to avoid incompleteness (e.g. Scholtz et al. 2018).

6 CONCLUSION

We measure the $R_{\rm MS}$ distribution of $z = 1$ AGN hosts split between low- and high-L_X AGNs separated at $L_X = 2 \times 10^{43}$ erg s^{-1}. We use a sample of 541 X-ray selected AGNs from the COSMOS field for which we derive SFRs or upper limits and measure stellar masses (see Section 2). We perform MLE to infer the $R_{\rm MS}$ distribution of the two samples of AGN hosts incorporating upper limits and under the assumption that the $R_{\rm MS}$ distribution is parametrized as a log-normal distribution, identical to that of the MS of star-forming galaxies (see Section 3). Our main results show that, with this assumption, the $R_{\rm MS}$ distribution of higher L_X AGNs is narrower (i.e. smaller σ by a factor of 1.4) and peaks at a higher value of $R_{\rm MS}$ (i.e. higher μ by a factor of 3) than that of lower L_X AGNs (see Fig. 2). This suggests less diversity in the star-forming properties of higher L_X AGNs when compared to their lower L_X counterpart. We speculate that the larger diversity in the star-forming properties of lower L_X AGNs may arise from the relative ease of an SMBH to trigger a low-L_X AGN in comparison to triggering a higher L_X AGN. Furthermore, higher L_X AGNs have hosts with star-forming properties in better agreement with that of MS star-forming galaxies, indicating that higher L_X AGNs are more likely to reside in MS star-forming galaxies. We also investigate the relationship between SFR and L_X for our two distributions by measuring the change in the mean and the mode of SFR with L_X (see Section 4.2). We find that our mean and mode SFRs are consistent with the flat relationship found between SFR and L_X, and that the mode SFRs lie below that of the mean, with a larger difference between the mean and the mode at lower L_X (see Fig. 4). This is a consequence of the differences in the width of the distributions at low and high L_X with the mean SFR being affected at different levels by bright outliers in the low and high L_X samples.

ACKNOWLEDGEMENTS

We thank the anonymous referee. EB, JRM, and CT acknowledge STFC grant R/151397-11-1. EB thanks C.M. Harrison and J. Scholtz for useful discussions that helped improving the clarity of the results and discussion.

REFERENCES

Aird J., Coil A. L., Georgakakis A., Nandra K., Barro G., Pérez-González P. G., 2015, MNRAS, 451, 1892
Aird J., Coil A. L., Georgakakis A., 2017, MNRAS, 465, 3390
Aird J., Coil A. L., Georgakakis A., 2018a, preprint (arXiv:1810.04683)
Aird J., Coil A. L., Georgakakis A., 2018b, MNRAS, 474, 1225
Bernhard E., Mullaney J. R., Daddi E., Ciesla L., Schreiber C., 2016, MNRAS, 460, 902
Bernhard E., Mullaney J. R., Aird J., Hickox R. C., Jones M. L., Stanley F., Grimmett L. P., Daddi E., 2018, MNRAS, 476, 436
Chabrier G., 2003, PASP, 115, 763
Ciesla L. et al., 2015, A&A, 576, A10
Foreman-Mackey D., Hogg D. W., Lang D., Goodman J., 2013, PASP, 125, 306
Gebhardt K. et al., 2000, ApJ, 539, L13
Georgakakis A. et al., 2014, MNRAS, 443, 3327
Goodman J., Weare J., 2010, Commun. Appl. Math. Comput. Sci., 5, 65
Harrison C. M., 2017, Nat. Astron., 1, 0165
Jin S. et al., 2018, ApJ, 864, 56
Kalfountzou E. et al., 2014, MNRAS, 442, 1181
Kauffmann G., Heckman T. M., 2009, MNRAS, 397, 135
Kennicutt R. C., Jr., 1998, ApJ, 498, 541
King A., 2003, ApJ, 596, L27
Lanzuisi G. et al., 2017, A&A, 602, A123
Larson D. et al., 2011, ApJS, 192, 16
Liu D. et al., 2018, ApJ, 853, 172
Lutz D. et al., 2011, A&A, 532, A90
Marchesi S. et al., 2016, ApJ, 817, 34
Mullaney J. R. et al., 2012, MNRAS, 419, 95
Mullaney J. R. et al., 2015, MNRAS, 453, L83
Mullaney J. R., Alexander D. M., Goulding A. D., Hickox R. C., 2011, MNRAS, 414, 1082
Noll S., Burgarella D., Giovannoli E., Buat V., Marcillac D., Muñoz-Mateos J. C., 2009, A&A, 507, 1793
Rosario D. J. et al., 2013, ApJ, 771, 63

Downloaded from https://academic.oup.com/mnrasl/article-abstract/483/1/L52/5212788 by University of Sheffield user on 07 March 2019

Sargent M. T., Béthermin M., Daddi E., Elbaz D., 2012, ApJ, 747, L31
Scholtz J. et al., 2018, MNRAS, 475, 1288
Schreiber C. et al., 2015, A&A, 575, A74
Stanley F. et al., 2017, MNRAS, 472, 2221
Stanley F., Harrison C. M., Alexander D. M., Swinbank A. M., Aird J. A., Del Moro A., Hickox R. C., Mullaney J. R., 2015, MNRAS, 453, 591
Wang T. et al., 2017, A&A, 601, A63

This paper has been typeset from a TEX/LATEX file prepared by the author.

Downloaded from https://academic.oup.com/mnrasl/article-abstract/483/1/L52/5212788 by University of Sheffield user on 07 March 2019